HIGHER ORDER SLIDING MODE PRECISION-LIMIT POSITIONING OF A DIRECT DRIVE SYSTEM

S.K.Spurgeon*, C.Hsieh †, C.Edwards*, C.L.Chen †

*Control and Instrumentation Research Group, University of Leicester, UK.
fax: +44 (0) 116 2522619
e-mail: eon@le.ac.uk
tel: +44 (0) 116 2522531

†Institute of Aeronautics and Astronautics, National Cheng Kung University, Taiwan.
fax: + 00 886 6 2389940
e-mail: chsieh@mail.ncku.edu.tw

Keywords: higher order sliding modes, position control, direct-drive system.

Abstract

This paper considers the application of a higher order sliding mode control algorithm to the problem of precision-limit positioning of a direct drive system in the presence of friction. Precision-limit positioning requires that the precision error is equal to the resolution of the sensor. Such high levels of control performance have not been generally considered possible because of the problems encountered in accurately modelling static friction. This paper employs a recently developed model of static friction and develops a higher order sliding mode position control algorithm. This algorithm does not require the output derivative (or velocity) to be measured or observed and merely employs the position error measurement to generate the control signal. This coincides with a fundamental requirement of precision limit positioning that only digital position measurement is used by the controller. Simulation and experimental results show good correlation. It is demonstrated that higher order sliding mode control is an appropriate technique for such precision limit position control.

1 Introduction

In recent years, higher order sliding mode controllers have received a great deal of attention in the literature [1-2,5,11-15]. This class of controllers is effectively a natural generalisation of classical sliding mode controllers. Such classical sliding mode controllers have sought to drive some appropriately defined switching function, s, to zero by employing a discontinuous control signal which effectively causes the first total derivative of s to be discontinuous. Higher order sliding mode controllers seek to render $s = \dot{s} = .. = s^{(r-1)} = 0$ and the discontinuity is seen to act on $s^{(r)}$. Classical sliding mode controllers are thus seen to be the special case of higher order sliding mode controllers obtained when r=1. The specific interest in higher order sliding mode controllers has occurred mainly as they provide a natural framework to smooth the discontinuity of the control signal that is present in classical sliding mode control. Although a number of papers in the literature consider theoretical issues in the area of higher order sliding mode controllers and a number of simulation studies exist, very little is reported on the practical application of such higher order sliding mode controllers.

This paper reports the application of a second order sliding mode controller to the precision limit positioning of the experimental facility shown in Figure 1. The plant is a direct drive DC torque motor mounted on ordinary ball bearings. The motor is driven by a linear amplifier. Two optical encoders with different resolutions are mounted to measure the rotor position. The resolution of the coarse encoder is 86,400 count/rev or, equivalently, 15 arcsec/count, while that of the fine encoder is 1,620,000 count/rev or, equivalently, 0.8 arcsec/count. The rotor angle is measured simultaneously by these two encoders. The outputs are compared to guarantee that the data obtained is correct. However, only one encoder is used in the feedback loop in each test. The data acqisition and control is accomplished by a PC-486/66 together with a D/A converter and an A/D converter. Both D/A and A/D converters have a resolution of 12 bits. The system is effectively a direct drive system in the presence of friction. The control objective is to ensure a zero-count steady state error with 100% repeatability . Consider

$$m\ddot{x} + c\dot{x} = u - \tau_f \qquad (1)$$

where x denotes the position, m denotes the mass, τ_f is the friction force, u is the control input and c is the damping coefficient in the slip phase. It is noted that, based on the usual Amonton-Coulomb friction model where static friction is essentially considered to be a dead-zone nonlinearity, any point $(x, \dot{x} = 0)$ in the state space is an equilibrium point when u is less than the maximum static friction. Therefore, the control u can be eliminated as the desired position is reached. However, this is not the case in practice. Experimental studies show that if a mass is moved a small distance in the operating range where static friction dominates, it will not stay there when the force is removed. This is effectively due to a nonlinear spring retraction. This also happens in a positioning system. The control force *u* becomes small as the mass *m* gets close to the desired position. It finally gets stuck due to static friction. The point it sticks at is usually not exactly the desired set point. In such a positioning system, the behaviour switches from that shown in Figure 2(a) to 2(b) as will be described in the next section. As the plastic module gets work hardened, the behaviour of the system is very close to that of a mass-spring-damper system. Therefore, to stay at the desired position, say x_d , a final holding force to compensate the spring force is required. If this force is removed, the mass bounces back and leaves the desired position. Although the system given in (1) looks simple, it, in fact, consists of two different systems: a type-1 slip system and a type-0 stick system. Since the two systems are quite different, it is natural to consider applying different control strategies for different phases to achieve a good response and this dual mode control philosophy has been reported in the literature, see for example [6]. Control design for coarse positioning in the slip phase has been well developed throughout the control literature. This study initially thought to concentrate on fine positioning in the stick phase using higher order sliding mode techniques. However, as will be seen from the experimental results, the single controller developed for the stick phase yields good performance in the slip phase also. This simplifies the controller design and implementation. The outline of the paper is as follows. Section 2 describes the friction model. The higher order sliding mode control design approach is covered in section 3. Simulation and experimental results are presented in section 4.

2 Description of Friction Model

The friction model developed in [8] as shown in Figure 2(a) is used for this study. The model consists of four elements - a plastic module, a nonlinear spring module, a viscous damper and a hook. These elements are assumed massless. During the slip phase, the tangential contacting force between the hook and ground can be described as a function of velocity. Such a representation describes the dynamic friction and has been proposed by many investigators. During the so-called pre-sliding motion[1], the hook sticks at the position where it is, and this model is reduced to that shown in Figure 2(b). In this model, the damper *c* is a standard linear damper and the nonlinear spring module and plastic module are as described below.

[1] The term pre-sliding is used here to describe a fundamental property of the friction dynamics and is not related to the sliding mode control technique used here.

Nonlinear spring module: Consider the nonlinear spring shown in Figure 3. Let σ_s be the applied external force and x_s be the elongation then the relation between σ_s and x_s follows the Preisach type hysteresis with loop congruency being obeyed in both the input and output senses. It has been shown in [7] that, for such hysteresis, the equation of each branch of the motion can be expressed as

$$\frac{d\sigma_s}{dx_s} = h(|x_s - x_r|) \qquad (2)$$

where $h(\cdot)$ is a nonnegative monotonically non-increasing function and x_r is the active reverse point, i. e., the starting point of the current branch of motion. It is noted that the slope at each point is a function of the relative absolute change of x_s with respect to the active reverse point, in contrast to other models [3,4]. An appropriate expression for $h(\cdot)$ in the pre-sliding motion is

$$\frac{d\sigma_s}{dx_s} = k_1 + k_2 e^{-\beta|x_s - x_r|} \qquad (3)$$

where k_1, k_2 and β are positive scalars. A typical response of the nonlinear spring is shown in Figure 4. If the hysteresis is treated as a spring then $h(\cdot)$ can be considered as the spring constant. For very small displacements, the nonlinear spring can be linearized.

Plastic module: Consider the plastic module shown in Figure 5. Let σ be the applied force and x_p be the extension, then it follows that:

$$\begin{cases} \dot{x}_h = \begin{cases} \alpha(f(|\sigma|) - x_h), & if\ f(|\sigma|) > x_h \\ 0 & , \ otherwise \end{cases} \\ \dot{x}_p = \operatorname{sgn}(\sigma)\dot{x}_h \end{cases} \qquad (4)$$

where α is a positive scalar and *f(s)* is a monotonically increasing function with *f(0) = 0* and $\left.\frac{df(s)}{ds}\right|_{s=0} = 0$. In this model, x_h is monotonically non-decreasing and stands for the accumulated work hardening and x_p is the final plastic deformation. It is noted that when $f(|\sigma|) > x_h$, new plastic deformation occurs. This deformation is referred to as creep motion. On the other hand, if $f(|\sigma|) \le x_h$, there is no new deformation. The module is work hardened. As a result, $f(|\sigma|)$ stands for the maximum amount of work hardening corresponding to the applied force σ. An appropriate expression for *f* is $f(|\sigma|) = \frac{|\sigma^n|}{\lambda}$, where *n > 1* and $\lambda > 0$ are both constants. A typical response of the plastic module is shown in Figure 6.

The pre-sliding motion is a combination of these modules as shown in Figure 2(b). Corresponding experimental and simulation results have been compared in [8]. They show very good consistency.

3. Higher Order Sliding Mode Control

Sliding Mode Control (SMC) is known to be a robust control method that is appropriate for controlling uncertain systems. High robustness is exhibited against external disturbances, measurement error and unmodelled plant dynamics. It is also relatively straightforward to implement the resulting algorithms. Fundamentally, sliding mode control design is a two stage process. Firstly, the sliding manifold is designed. The requirement here is that the zero dynamics of the system with respect to a suitable output (the sliding variable, s) exhibits desired behaviour. Secondly, a control is designed to force the system trajectories to the designed sliding manifold, which is defined as $s = 0$, and ensure they remain there. In classical sliding mode control, the sliding variable is selected such that it has relative degree one with respect to the control. The control then acts on the first derivative (with respect to time) of the sliding variable ($\dot{s}$) to keep the system trajectories in the sliding set $s = 0$. Essentially, the discontinuous control signal acts on the first derivative of s. This condition effectively limits the choice of sliding variable.

The concept of higher order sliding mode control has recently gained a great deal of attention in the literature [5,12,16]. In higher order sliding mode control, the control acts on higher derivatives of the sliding variable. For example, the case of second order sliding mode control corresponds to the control acting on the second derivative of the sliding variable, namely $\ddot{s}$, and the sliding set is defined as $s = \dot{s} = 0$. It is readily seen that such a higher order sliding mode control provides a natural means to alleviate one of the perceived problems of classical sliding mode control, namely chattering of the control signal. Several such second order sliding algorithms have been presented in the literature [1,2,11,13,14]. In [11,13] 2-sliding algorithms were presented to stabilise second order uncertain nonlinear systems but these use knowledge of the output-derivative, $\dot{s}$, to implement so called twisting or drift algorithms. The super twisting algorithm in [11] does not require this output derivative to be measured. However, it has been developed for systems with relative degree one with respect to the input and, if applied to systems of relative degree two, develops limit cycle behaviour; the conditions for controller parameter selection are no longer valid.

In [1,2] an optimised version of the twisting algorithm was presented. However, this requires at least knowledge of the sign of the output-derivative which is implemented by incorporating a memory element into the controller. A new second order sliding mode control algorithm has recently been developed for systems of relative degree two with respect to the input in which $\dot{s}$ is not measured or observed [10]. Further, it is not assumed that the sign of $\dot{s}$ is detectable. To describe the algorithm, consider a second order single input single output (SISO) system of the following type

$$\begin{aligned} \dot{y}_1 &= y_2 \\ \dot{y}_2 &= f(y_1, y_2, t) + g(y_1, y_2, t)u \end{aligned} \tag{5}$$

where $0 \le |f(.)| \le F$ and $0 < G_{\min} \le |g(.)| \le G_{\max}$ are uncertain, bounded functions. It is required to stabilize the output y_1 of this system using a sliding mode control with the condition that neither measured nor observed y_2 is available to the controller. The system output y_1 can be considered as the suitable sliding variable. The following second order sliding algorithm is suggested to steer y_1 to zero exponentially and achieve the control task. The algorithm is defined by the following control law.

$$\begin{aligned} u &= u_1(t) + u_2(t) \\ u_1 &= -\lambda \operatorname{sign}(y_1) \\ \dot{u}_2 &= \begin{cases} -ku & |u| > u_0 \\ -W\operatorname{sign}(y_1) & \text{otherwise} \end{cases} \end{aligned} \tag{6}$$

where $\lambda > u_0 > \dfrac{F}{G_{\min}}, k > 0, W \ge 0$. This algorithm is here applied to the fine position control problem described in Section 2. The bounds on $|g(.)|$ depend only upon the range of variation of $1/m$ where m is the mass. The bounds on $|f(.)|$ depend on variation in c, the damping coefficient in the slip phase, the range of variation of $1/m$, k_1, k_2 and the magnitude of the friction torque. The accurate simulation model of the pre-sliding behaviour was used to determine these bounds and hence evaluate the controller parameters. It should be noted that the integral term in this higher order sliding mode control algorithm is needed to give the holding force required in the steady-state for precision limit positioning.

4 Experimental Results

The system used in this research to conduct experiments is shown in Figure 1. Experimental procedures follow those described in [7]. Figure 8 shows the simulation results obtained from applying a 1 count, 5 counts and 10 counts step command to the pre-sliding system simulation model. The precision limit positioning task is accomplished in each case. Figure 9 shows the corresponding experimental results. Here the digital output from the coarse encoder is used by the control signal. Again the precision limit positioning task is accomplished. Figure 10 shows a large movement task. It is seen that the designed second order sliding mode controller is able to accomplish precision limit positioning in this phase of movement also. As was commented earlier, previous studies would consider a two stage controller design for each phase of motion. Note that the second order sliding mode controller was implemented with exactly the same algorithm and identical sets of parameters for both phases of motion. Traditional sliding mode control algorithms, effectively first order sliding modes, do not necessarily have the integral term required to prescribe the holding force in the steady state.

5 Concluding Remarks

The design of a second order sliding mode control system for precision limit positioning in the presence of friction has been discussed. A second order sliding mode control algorithm has been employed that does not require measurement or estimation of the velocity. Implementation results have been presented and the performance of the second order sliding mode controller has been found to be as predicted by simulation studies. It has been shown that the second order sliding mode controller is straightforward to tune and implement and is capable of giving good performance in both the pre-sliding and sliding phases of operation. The results have been achieved using position error measurement only with no measurement or estimation of velocity.

Acknowledgements

This work would not have been possible without the award of a UK-Taiwan Joint Project Grant from The Royal Society, UK and the National Science Council (NSC90-2911-I-006-007), Taiwan. This support is most gratefully acknowledged.

References

[1] G. Bartolini, A. Ferrara, A. Levant, and E. Usai, "On second order sliding mode controllers", in K.D. Young and U.Ozguner, editors, Variable Structure Systems, Sliding Mode and Nonlinear Control, volume 247 of Lecture Notes in Control and Information Sciences, pp. 329--350. Springer, London, (1994).

[2] G. Bartolini, A. Ferrara, and E. Usai, " Application of a sub-optimal discontinuous control algorithm for uncertain second order systems", *Int. J. Robust and Nonlinear Control*, **7**, pp. 299-319, (1997).

[3] C. Canudas de Wit, H. Olsson, K.J. Aström, and P. Lishinsky, "A new model for control of systems with friction". *IEEE Trans. on Automatic Control*, **AC(3)**, pp. 419-425, (1995).

[4] P.R. Dahl, "Solid friction damping of mechanical vibrations", *AIAA Journal*, **14(12)**, pp. 1675-1682, (1976).

[5] S.V. Emel'yanov, S.K. Korovin, and A. Levant, "High order sliding modes in control systems", *Computational Mathematics and Modelling*, **7(3)**, pp. 294-318, (1996).

[6] S. Futami, A. Furutani, and S. Yoshida, "Nanometer positioning and its micro-dynamics", *Nanotechnology*, **1**, pp. 31-37, (1990).

[7] T.Y. Lin, Y.-C. Pan, and C. Hsieh, "Precision-limit positioning of direct drive systems with the existence of friction", *Control Engineering Practice*, to appear.

[8] C. Hsieh, and Y.-C. Pan, "Dynamic behavior and modelling of the pre-sliding static friction", Wear, **242(1-2)**, pp. 1-17, (2000).

[9] C. Hsieh, and T.-Y. Lin, "Modeling of the Preisach Hysteresis Using the Switched System Approach", *Trans. of the Aero. and Astro. Society of the R.O.C.*, to appear.

[10] M.K. Khan, S.K. Spurgeon, and A. Levant, "Simple output feedback 2-sliding controller for systems of relative degree two", Proceedings of ECC 2003.

[11] A. Levant, "Sliding order and sliding accuracy in sliding mode control", *Int. J. Control*, **58(6)**, pp. 1247-1263, (1993).

[12] A. Levant, and L. Fridman, " Higher order sliding modes as a natural phenomenon in control theory", in E. Garofalo and L. Glielmo, editors, Robust control via variable structure and Lyapunov Techniques, volume 217 of Lecture Notes in Control and Optimization, pp. 107-133. Springer, London, (1996).

[13] A. Levant, "Higher order sliding: collection of design tools", In *Proc. European Control Conference*, Brussels, (1997).

[14] A. Levant, "Robust exact differentiation via sliding mode technique", *Automatica*, **34**, 3, pp. 379-384, (1998).

[15] A. Levant, "Universal single-input-single-output (SISO) sliding mode controllers with finite time convergence", *IEEE Trans. Automatic Control*, **46(9)**, pp. 1447-1451, (2001).

[16] H. Sira-Ramirez, "On the dynamic sliding mode control of nonlinear systems", *Int. J. Control*, **57**, 5, pp. 1039-1061, (1993).

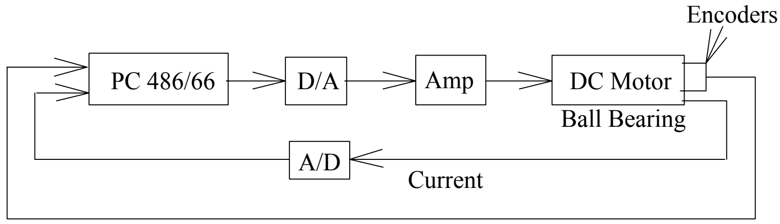

Figure 1(a) Block diagram of system hardware

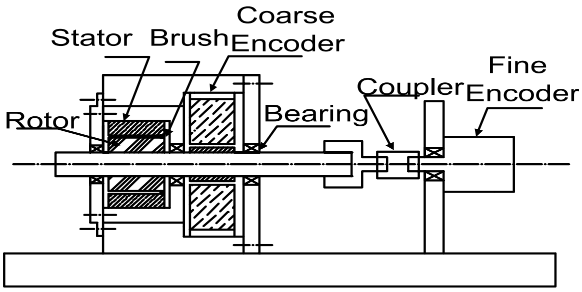

Figure 1(b) Schematic diagram of the test platform

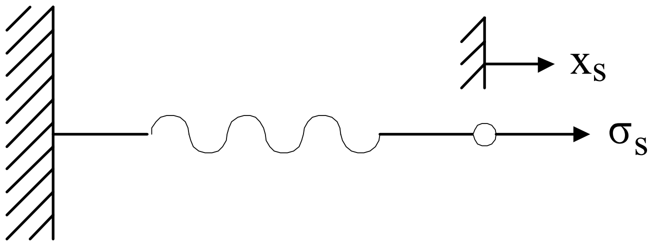

Figure 3. Nonlinear spring module

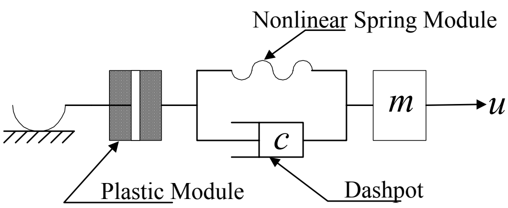

Figure 2(a) Model of friction

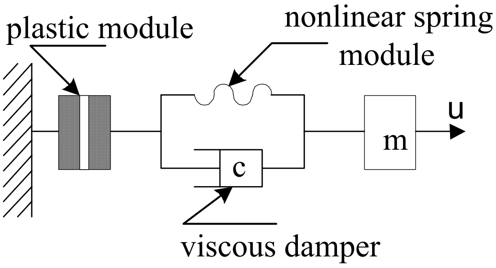

Figure 2(b) Static Friction Model

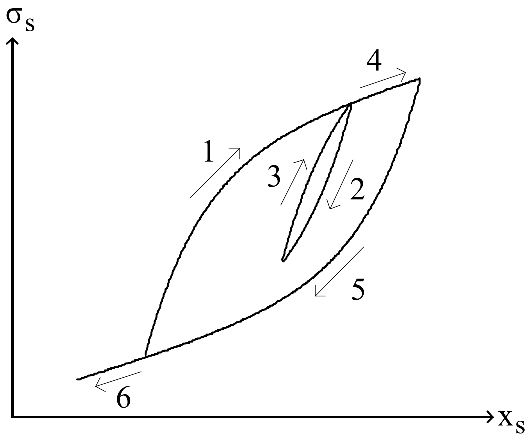

Figure 4 Typical response of the hysteresis non-linearity of the nonlinear spring module

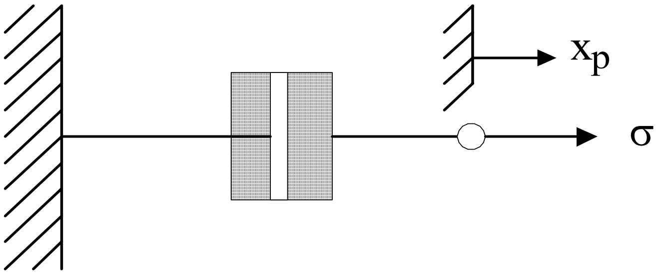

Figure 5. Plastic module

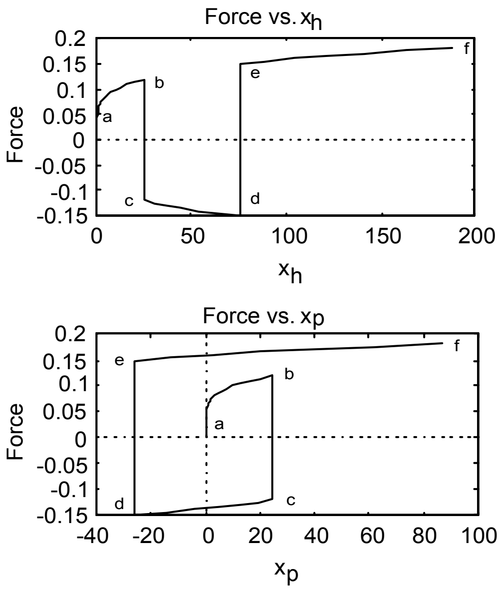

Figure 6. Typical response of the plastic module

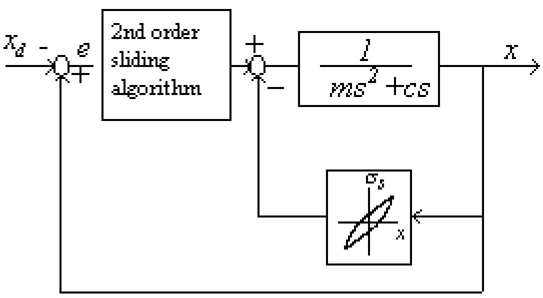

Figure 7. Control system block diagram

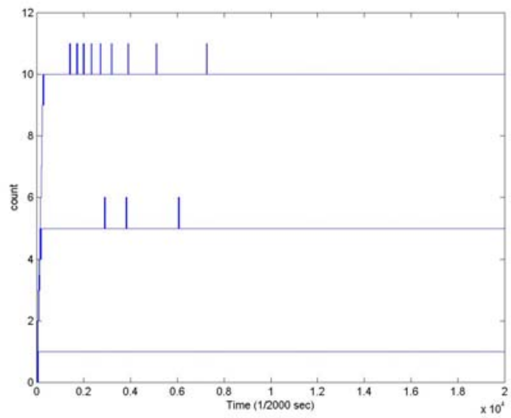

Figure 8 Simulated step responses (1 count, 5 counts, 10 counts)

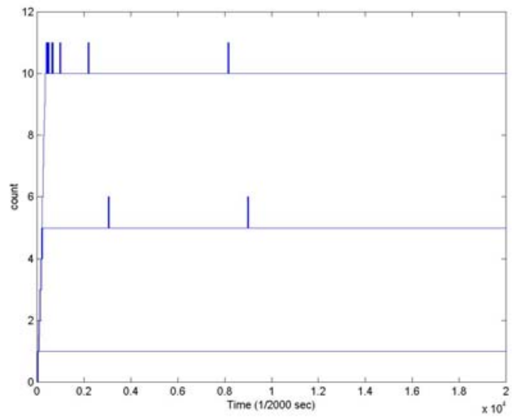

Figure 9 Experimentally measured step responses (1 count, 5 counts, 10 counts)

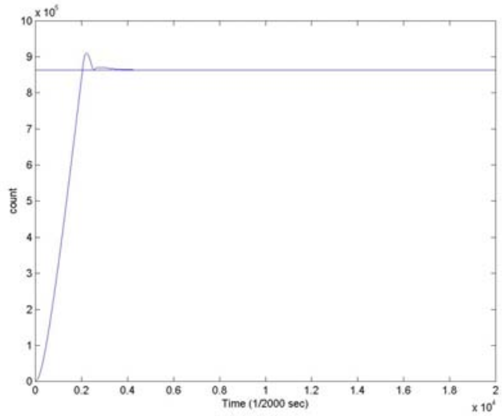

Figure 10 Experimentally measured step response (864000 counts)